

# Micro-clamps for precise positioning of 120° silicon double mirrors in a MOEMS gyroscope

Thalke Niesel\*, Andreas Dietzel

Technische Universität Braunschweig, Institut für Mikrotechnik, Alte Salzdahlumer Straße 203, 38124 Braunschweig, Germany

\*corresponding author

e-mail: [t.niesel@tu-braunschweig.de](mailto:t.niesel@tu-braunschweig.de)

phone: +49(0)531/391-9759

fax: +49(0)531/391-9751

## Keywords

Silicon double mirror; micro-clamps; MOEMS; optical gyroscope;

## Abstract

Micro silicon double mirrors have been developed specifically for the design of a novel micro-optical gyroscope. By using wafers with a well-defined angular offset to the (100) plane, an etching angle of 60° can be achieved by wet-chemical etching with KOH. Two likewise structured wafers are connected by means of silicon direct bonding and consequently form 120° double mirrors. A big advantage of these double mirrors is that inaccuracies during assembly onto a micro optical table, such as shifts in the x- and y-direction and twists around the vertical axis are compensated by the mirror and a fixed angle of reflection is maintained. Assembly tolerances for the other two rotational degrees of freedom cannot be compensated in this way yet and a precise rotational alignment of the mirror elements in an optical resonator is still required. Therefore a micro clamping device was developed that can be used in the assembly of a micro-optical gyroscope. The key elements are micro spring structures integrated in the micro-optical table which can be pushed back to allow the insertion of the mirror elements and press the mirrors against two lithographically defined mechanical stops. Various designs of clamping devices were fabricated and their suitability in an optical gyroscope was evaluated.

## 1. Introduction

Inertial navigation devices are indispensable elements in our technological world. We find them in cars, ships and planes, as well as satellites, autonomous robots and gaming devices. They can provide a complete motion vector and they are reliable, robust against external interference. Through continuous developments high precision inertial measurement units (IMU) become smaller and lighter. This makes them interesting for new applications with special demands on the weight, for example small autonomous objects like drones. A complete IMU is usually composed of three accelerometers and three gyroscopes, one for each axis of translational and rotational motion, so any motion can be fully tracked. The gyroscopes are used to measure the rate of rotation and allow determining the attitude angles by integration. With the integration, however, the measurement errors in the rate of rotation accumulate over time. Therefore it is crucial to reduce measurement errors. A micro-optical gyroscope to be used as an angular rate sensor for navigation purposes should satisfy high demands on precision, stability and integrity. A new concept for a micro-optical gyroscope was developed that should be characterized by lower measurement tolerances when compared to well-known MEMS gyroscopes but should also be much smaller than conventional optical gyroscopes. In the course of the development of a miniaturized optical gyroscope, silicon mirrors and suitable positioning methods were investigated that allow to reduce or compensate inaccuracies that can occur during the system assembly. Double mirrors which can compensate for alignment inaccuracies are a key element and have already been presented [1]. Here, novel micro clamps for mounting these mirrors are presented. They shall secure high precision for the degrees of freedom which cannot be compensated by the double mirror itself.

## 2. Concept of the MOEMS gyroscope

In our recent work, a concept for building a new micro-optical gyroscope was developed in which structural elements already prevent assembly inaccuracies leading to malfunctioning of the system. Key elements are silicon-double mirrors that guarantee an angle of reflection unaffected by variations in the incident direction. Integrated waveguides provide the coupling and outcoupling of laser radiation into the optical resonator. Figure 1 shows a test platform with mirrors mounted onto the micro optical table with optical waveguides made from SU-8, which direct the laser radiation in the resonator. Here clamping devices are not yet integrated. To test the mirror and the resonator, an external laser is used. A laser beam can be coupled directly over the edge into the optical waveguide on the silicon. Likewise, the outcoupled light is sent to an external detector. The individual components are described in more detail below.

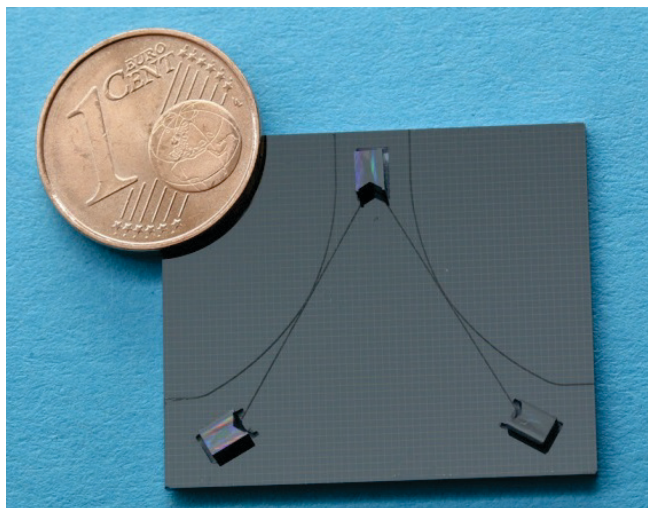


**Figure 1:** Ring resonator consisting of micro-optical table made from silicon, micro mirrors which are mounted in dry-etched mirror pits and optical waveguides made from SU-8.

### 2.1. The double mirror

By using specially prepared off-axis wafers with an angular alignment of  $5.3^\circ$  relative to the (100) plane wet-chemical KOH/IPA etching results in {111} facets at angles of  $60^\circ$ . These etch facets determined by the crystallography with high precision are used as mirrors. The angle of the opposite {111} flanks are accordingly smaller (about  $49^\circ$ ). Double mirrors with a  $120^\circ$  angle are formed by connecting two structured silicon wafers by direct bonding. After bonding for 30 min at  $1000^\circ\text{C}$ , the stack is cut with a saw into individual mirror elements with dimensions of  $2\text{ mm} \times 2\text{ mm} \times 3\text{ mm}$ . In order to improve the reflection characteristics, the mirror surfaces may additionally be metal coated. At present sputtered gold, chromium, silver and titanium are tested as coating materials. The details of the concept and the fabrication of the micro double mirrors have been described earlier [1].

### 2.2. Optical waveguide

Optical waveguides made of SU-8 2000 and SU-8 3000 or OrmoCore and OrmoClad are used for the gyroscope's resonator to guide and to couple/outcouple the laser beam. In Fig. 1 optical waveguides from SU-8 are shown made, which guide the light from the laser into the resonator and from there also out onto a laser diode connected to readout electronics. The light coupling is achieved by proximity couplers. Two waveguides are running parallel to each other over a certain distance with a short gap in between ( $500\text{ nm}$  up to  $2\text{ }\mu\text{m}$ ). If the waveguides run close enough to each other the light couples between parallel waveguides by overlapping of the evanescent fields. Early descriptions of this effect can be found in [2]. However, coupling can also occur when waveguides are connected by residual layers between the waveguides. Thereby coupling is possible even at greater distances between the waveguides which can be achieved through manufacture with conventional lithography. The operation and further explanations of the coupler used here can be found in [3]. The coupling can be inversed, so that this mechanism is used for incoupling and for outshapecoupling. This solution allows to shape the light prior to entering into the resonator and to splitting the beam for both directions, clockwise and counterclockwise.

## 3. The concept of micro-clamps

The mirror elements must be arranged as an optical resonator for the gyroscope. Therefore, the individual elements must be mounted on a platform on which the planar waveguides are already micro fabricated. To fix the mirrors in well-defined positions, clamping devices have been developed which press the mirror elements against lithographically defined corners. Similar spring structures have been used earlier for micro-grippers so the behavior of the design is well-known [4] - [7]. The structure has been adapted for a clamping unit, while retaining its original functional elements. It is assumed that the mechanical behavior of these clamps is comparable with the grippers, so no FEM simulations were necessary. Figure 2 shows the model of a clamping device with a thereby mounted double mirror element. This clamping element shall hold a mirror element in position but shall also correct inaccuracies resulting from assembly processes. In this figure geometrical parameters, structural width, spring path and preload which characterize the clamping device are illustrated, too. The preload is the distance between mirror backside and the position when the spring is unloading without a mirror element.

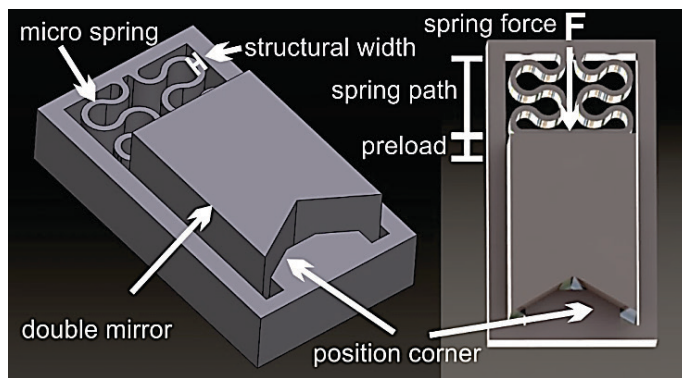
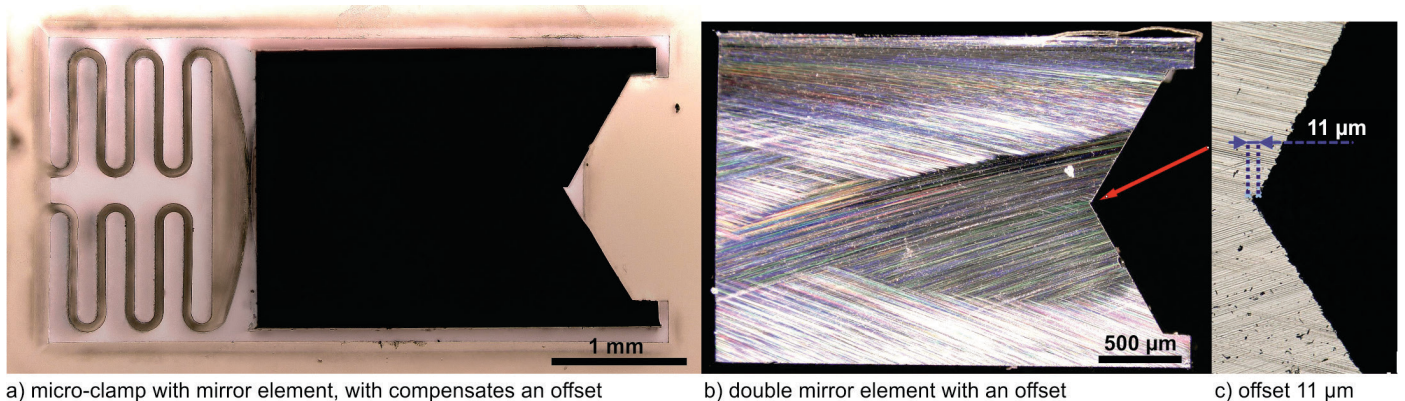


**Figure 2:** Different views of a CAD model for a clamping device illustrating also some geometric parameters characterizing different designs.

The spring stiffness depends on the material and the geometry of the spring. This spring structure is not a simple bending beam, but each section of the meander structure may in a simplistic view be considered as such. The flexural rigidity of a bending beam is the product of the modulus of elasticity  $E$  of the material and the area moment of inertia  $I$  of the beam cross section. When loading the spring in a direction parallel to the wafer surface, the flexural rigidity is proportional to the wafer thickness but goes with the third power of the structural width. If dimensions of the spring do not change the spring stiffness changes only in linear dependence on the modulus of elasticity  $E$  of the material the spring is constructed of. The modulus of elasticity of crystalline silicon is not isotropic but ranges between 130-188 GPa. SU-8 2000 and also SU-8 3000 are specified with  $E = 2$  GPa in the material data sheet. Earlier bending measurements with SU-8 processed at different drying times and temperatures showed that the modulus of elasticity varies in the range between 3-6 GPa [4], [6]. A precise prediction of force-displacement characteristic has to take corner and edge effects and potentially also hysteretic material effects into account which probably requires detailed FEM analysis. However, the mentioned dependencies may be sufficient to allow scaling of the clamps to adapt them to specific design goals. This is to verify one of the results expected from experimental testing of micro fabricated prototype spring structures.

Fig. 3a shows a micro fabricated micro-clamp fixing a mirror element. Fig. 3b) shows a bottom view of the mirror element and the arrow indicates where a picture at higher magnification (Fig. 3c) was taken in which a wafer to wafer offset of  $11\ \mu\text{m}$  is visible. This offset can be a result of inaccurate alignment during wafer bonding but also of different etching depths in the two silicon wafers. The angle between the two etched sidewalls is unaffected, however, and remains at  $120^\circ$ . The corners to which the mirrors are pressed by the spring elements are designed with a flat so that this offset has no influence on the resonator.



a) micro-clamp with mirror element, with compensates an offset  
**Figure 3:** Clamping element to compensate for an offset.

### 3.1. Design parameters

Spring structures of different styles and dimensions were manufactured and tested for their suitability in a micro-optical gyroscope. The silicon structures were formed by dry etching in an ICP-etcher and the SU-8 structures were manufactured by deep lithography.

Fig. 4 shows a selection of different clamping elements. The springs differ in material, shape of the spring meander pattern, structural width of the meandering spring, length of spring path, length of the spring preload and shape of the surface in contact to the mirror backside.



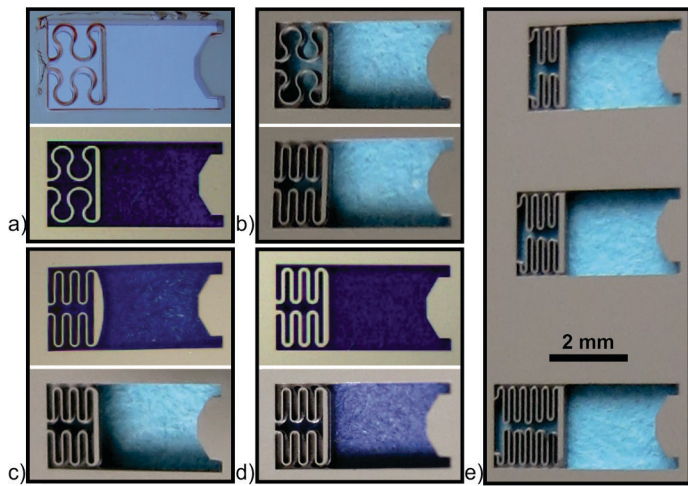


**Figure 4:** Clamping elements with parameter variations; a) Material SU-8 vs. silicon, b) spring structure large vs. fine, c) shape of the contact area round vs. plane, d) structural width 100  $\mu\text{m}$  vs. 50  $\mu\text{m}$ , e) spring path 500  $\mu\text{m}$  vs. 1000  $\mu\text{m}$  vs. 2000  $\mu\text{m}$ .

### 3.2 Micro manufacture of clamping elements in silicon

Wafers with a thickness of 360  $\mu\text{m}$ , 480  $\mu\text{m}$  and 1000  $\mu\text{m}$  were used for the silicon clamping elements. A variation in the spring stiffness resulted from the variations of the thickness. With increasing wafer thickness the corner stop facets to which the mirror elements are pressed increase. Larger corner facets reduce the risk that the mirror elements can tilt. The masking layer for the ICP dry etch process consists of a 200 nm thick chromium layer which is applied on both sides and subsequently patterned photolithographically. Using the ICP-multiplex system from STS the wafers are locally etched down to half the thickness in a DRIE process (Deep Reactive Ion Etching) and then flipped to etch through the entire wafer thickness. After removing the masking layer in acidic chrome etch-solution the clamping devices are ready for mirror mounting.

A particular challenge is the structuring of the 1000  $\mu\text{m}$  thick wafers due to the increased aspect ratio (20:1) which some designs demand at critical lateral dimensions. As a consequence the etch rate is lower for structures with such critical dimensions and not all structures could fully be realized with a comparable quality in one process on the same wafer. Figure 5 a) and b) show structures obtained on the same  $t = 1000 \mu\text{m}$  thick wafer. The nominal structural width dimensions  $t$  of the clamping elements is given. It can be clearly seen that wider and smaller gaps between the spring structures are etched at different rates. At a nominal spring structural width of 100  $\mu\text{m}$ , the wide curved spring is already released, whereas the spaces between the closely curved spring are still connected (Fig. 5a). However, the more filigree spring with a nominal structural width of 60  $\mu\text{m}$  already disappeared for the most part due to undercutting (Fig. 5b). In the case of 1000  $\mu\text{m}$  thick wafers the etching process must be optimized individually for different structure dimensions. The situation is easier with thinner wafers; here both the small spring widths (Fig. 5c) as well as the larger spring widths can be realized in one process on the same wafer. Anyway, for a final clamp design the process can be adjusted to the chosen structure sizes.

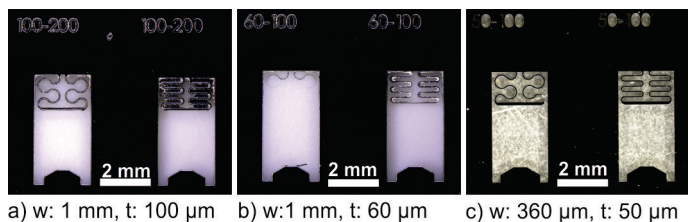


**Figure 5:** dry etching silicon structures,  $w$  = wafer thickness,  $t$  = spring structural width.

### 3.3 Micro manufacture of clamping elements in SU-8

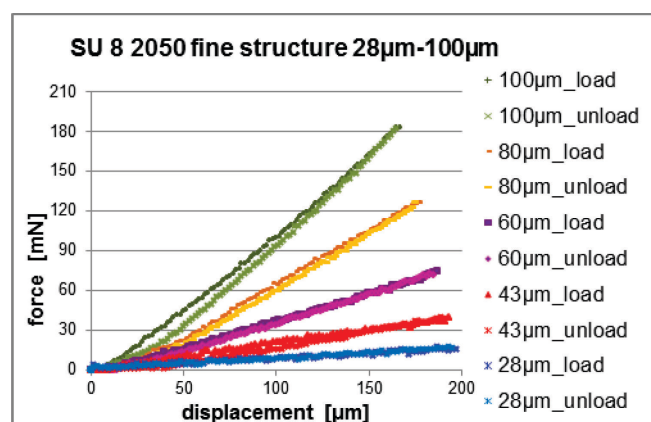
SU-8 clamping systems were processed in two different thicknesses (550 - 600  $\mu\text{m}$  and 950 - 1000  $\mu\text{m}$ ). Two resist series; SU-8 2050 and SU-8 3050 were tested. Thick glass wafers were used as temporary carrier substrates for the SU-8 structures 700  $\mu\text{m}$ . These were coated with a 2  $\mu\text{m}$  thick copper sacrificial layer to allow peeling the SU-8 from the glass substrate in one piece. In order to achieve the desired height of the SU-8 structures, a multi-layer process was carried out, wherein each layer has a thickness of about 160  $\mu\text{m}$ . Through several heating and cooling steps that lasted several hours, a uniform stress-free drying can be realized. After spin coating each layer is leveled on a hotplate at 50° C for 45 minutes with a glass cover. Following the removal of the glass cover the hotplate is then ramped up slowly to the softbake temperature of 95° C which is then held for 5 hours. Afterwards the wafer is allowed to cool down to room temperature overnight while remaining on the hotplate. This process is repeated for each additional layer, but the drying time is increased by one hour for each new layer. After the photolithographic patterning of the different layers, the whole layer structure is separated from the glass wafer by etching the copper layer. The resulting spring structures with dimensions comparable to the ones made from silicon substrates can be moved freely.

## 4. Measured spring characteristics

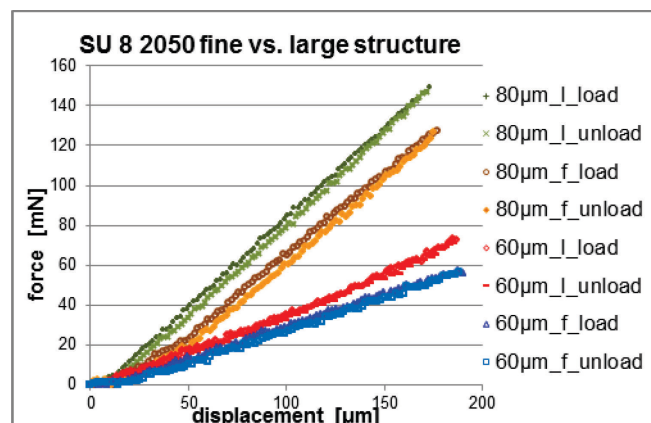
To investigate the influence of design variations on the mechanical behavior of the clamps, force-displacement measurements were conducted. The clamping units were cut into smaller samples which were affixed in a holder. A probe tip attached to a 0,5 N force sensor (me-systeme.de KD78 0,5 N) was positioned in the pit in front of the spring. This force sensor was situated on a linear axis (PI M-531.5IM) which was moved in steps of 2  $\mu\text{m}$  thus deflecting the spring. After reaching a deflection of 200  $\mu\text{m}$  the spring was relieved again in small steps. These measurements were automated by a LabView program, which recorded the force and displacement values. Each micro spring sample was measured over three cycles (load-unload) and average values are shown in the graphs in Figure 6. Figure 6a) compares different spring widths in SU-8 2050 at a thickness of 1000  $\mu\text{m}$ . Spring widths of 100  $\mu\text{m}$ , 80  $\mu\text{m}$ , 60  $\mu\text{m}$ , 43  $\mu\text{m}$  and 28  $\mu\text{m}$  are compared. All springs show an almost linear response at load and unload. The weak hysteretic effect which can be observed in the graphs is a result of the experimental arrangement. In some cases, the sample has a little play in the holder and can be pushed forward during loading. That explains why the load curves exhibit higher values than the unloading curves, especially if greater forces were applied. However, for the purpose of determining the influence of variations in the spring design this effect can be neglected. By widening the spring structural width  $t$  the clamping force increases. As discussed earlier in paragraph 3 the spring constant should scale approximately with third power of  $t$ . In Figure 6b) values for the large spring structure and the finer (see Fig 4 b) one are plotted. 80  $\mu\text{m}$  and 60  $\mu\text{m}$  structure widths are compared for both structures. The required forces are

approximately  $(\frac{8}{6})^3$  times larger for the wider structure clamps as expected by the third power law. It also turns out that the large spring structure with the same dimensions for the same displacement requires about 20% more deflection force compared with the finer one. Figure 6c) shows a comparison of measured force-displacement curves for micro-clamps made from SU8 and Silicon. The measurements are made with  $t = 80 \mu\text{m}$  wide clamps in all cases. Clamps from SU-8 2050 and from SU-8 3050 in a thickness of 1000  $\mu\text{m}$ , and silicon springs in thicknesses of 360  $\mu\text{m}$  and 500  $\mu\text{m}$  are measured. It shows that for the structures of SU-8 3050 a 30% higher force is required compared to the structures of SU-8 2050 when displaced at the same distance. In comparison, 17 times as much force as for SU-8 is required for silicon of half the thickness. Since the spring constant scales linearly with wafer thickness and with  $E$  modulus this result is in accordance with the expected behavior as described in paragraph 3.

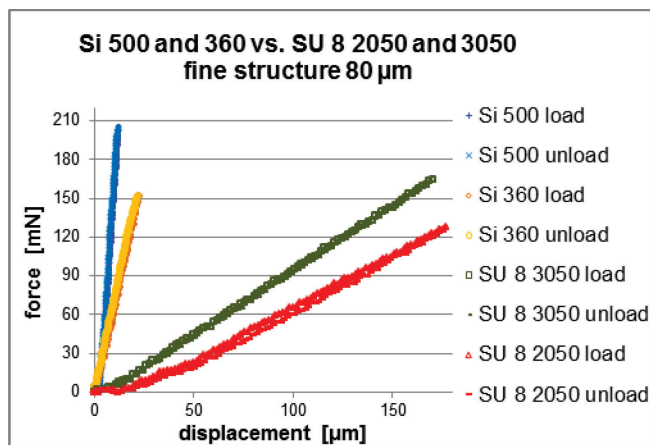
The measurements confirm that the clamping force of the springs can be set individually by selecting the design parameters. It has been found that larger spring travel helps in the manual assembly (insertion) process for the mirror elements. To test the clamping devices during movement of the gyroscope, clamped levels were positioned on a turntable and rotated at up to 360  $^\circ/\text{min}$ . At this speed no remaining changes in the position of the mirrors could be detected after rotation.



a) Different spring thicknesses



b) Comparison between fine and large structures



c) Material; silicon and both SU-8 series

**Figure 6:** Force-displacement measurements from different spring designs and materials (The legend of the graph is sorted according to the plotted lines from top to bottom.).

In view of a robust gyroscope design, the silicon clamps are preferred to the SU-8 clamps. With equal dimensions in spring height and width, the forces of silicon clamp are about 30 times bigger and silicon material is free of degradation and hysteretic effects. The forces provided by the SU-8 clamps together with friction forces occurring between the mirror and the clamping frame in the micro optical platform are sufficient to hold the mirror in its position and also to keep it in position even after rotation. But the frictional forces occurring at the interfaces between micro mirror and clamp frame are strong enough so that the micro mirror may persist also in misaligned position and the clamping force does not overcome the frictional force with the result that the mirror does not fully align against the facets of the alignment corner.

## 5. Conclusion and Outlook

In this paper, the concept for the implementation of a micro-optical resonator gyroscope is described from which the necessity of micro alignment for two rotational axes becomes obvious. Micro clamps are presented, which allow aligned positioning and fixing of the double mirror elements in order to compensate initial rotational misalignments in the assembly of the resonator. The micro fabrication of clamps from silicon and SU-8 is portrayed and the scaling of the spring stiffness and clamping forces with geometrical and material parameters confirmed. In the future even stiffer micro spring structures will be investigated which can overcome all frictional forces during alignment. With the confirmed scaling rules of the micro clamps new designs can be developed in which the clamping force can be balanced against space consumption within the micro optical platform to still allow for a very compact gyroscope system.

## 6. Acknowledgements

The authors acknowledge the financial support from the Federal Ministry of Economics and Technology (BMWi) through the German Aerospace Center (DLR) under grant number FKZ 50 NA 1218 providing the frame for the described research.

## 7. References

- [1] T. Niesel, A. Dietzel, Fabrication of 120° silicon double mirrors robust against misalignment for use in micro optical gyroscopes, *Microelectronic Engineering* 121 (2014) 72–75, doi: 10.1016/j.mee.2014.03.035.
- [2] A. Yariv, Coupled-mode theory for guided-wave optics, *IEEE J.Quant. El.* QE-9 (1973), 919.
- [3] I. Leber, T. Niesel, A. Dietzel, Waveguide-coupling to be used in a micro optical laser gyroscope, *Proc. of SPIE* vol. 9577, *SPIE Optical Engineering + Applications*, SPIE (2015) ,95770O1-95770O8, doi: 10.1117/12.2189522.
- [4] S. Bütefisch, V. Seidemann, S. Büttgenbach, Novel micro-pneumatic actuator for MEMS, *Sensors an Actuators A: Physical* Vol. 97-98 (2002), 638-645, doi: 10.1016/S0924-4247(01)00843-3.
- [5] B. Hoxhold, S.Büttgenbach, Batch fabrication of micro grippers with integrated actuators, *Microsystem Technologies*, Vol. 14, Issue 12 (2008), 1917-1924, doi: 10.1007/S00542-008-0659-3.
- [6] S. Bütefisch, Entwicklung von Greifern für die automatisierte Montage hybrider Mikrosysteme, Dissertation, TU Braunschweig, Berichte aus der Mikro- und Feinwerktechnik, Shaker Verlag (2003),
- [7] B. Hoxhold, Mikrogreifer und aktive Mikromontagehilfsmittel mit integrierten Antrieben, Dissertation, TU Braunschweig, Berichte aus der Mikro- und Feinwerktechnik, Shaker Verlag (2011), 87-90.
- [8] R. Feng, R.J. Farris, The characterization of thermal and elastic constants for an epoxy photoresist SU8 coating, *Journal of Materials Science*, Vol. 37, Issue 22 (2002), 4793-4799, doi: 10.1023/A:1020862129948.